Study of electrical transport properties in perovskite solar cells based on MAPI grown by physical vapor deposition

Miguel Ángel Reinoso
Facultad de Ciencias e Ingeniería
Universidad Estatal de Milagro
Milagro, Ecuador
mreinosos@unemi.edu.ec

Hebert Alexander Gómez
Departamento de Física
Universidad Nacional de Colombia
Bogotá, Colombia
heagomezru@unal.edu.co

Gerardo Gordillo Guzmán
Departamento de Física
Universidad Nacional de Colombia
Bogotá, Colombia
ggordillog@unal.edu.co

***Abstract*—This work seeks to contribute to development of new photovoltaic materials to be used in low cost solar cells and low environmental impact. Special emphasis was placed on the study of electric transport properties in perovskite solar cells with structure FTO/ZnO/MAPI/P_3HT/Au, using impedance spectroscopy technique. MAPI ($CH_3NH_3PbI_3$) thin films were deposited by sequential evaporation and its thickness was varied between 300 and 600 nm. Through simulations of impedance curves, it was possible to model the electrical behavior of the cells, where simulated circuit elements values were found: R_0, R_{S1}, R_{S2}, C_g and C_S. From the above, the resistance at low frequencies R_{S1} has higher values than the component R_{S2} at high frequencies (HF) and since these have an inverse relationship with the recombination current $J_{rec,s}$ we can say that photocurrent losses by recombination are greater at HF.**

Keywords—electrical properties, impedance spectroscopy, perovskite solar cells, MAPI, physical vapor deposition

I. INTRODUCTION

Photocurrent in solar cells is limited by losses associated with different processes such as: recombination of electrons in surface states generated by incomplete bonds, recombination of carriers in interface states caused by mechanical stresses, due to decoupling of lattice constants between materials, recombination of electrons and holes in the active layer and space charge zone, charge transfer through potential barriers due to the difference in the work function of the materials.

Different characterization techniques study electric transport properties in solar cells; however, these have limitations such as complex equipment expensive. On the other hand, impedance spectroscopy requires a low-cost infrastructure and allows determining charge carriers (electrons and holes) mobility as well as parameters that give information about charge transfer at the interfaces and the processes responsible of photocurrent losses [1].

Impedance Spectroscopy (IS) has been widely used for the characterization of photovoltaic devices manufactured with different architectures [2, 3]. Its importance lies in the fact that it allows information on the mechanisms of electrical transport in the different components of the device.

The IS technique consists in applying on material an electrical potential (or voltage) as sinusoidal signal with variable frequency given by [1, 4, 5]:

$$V(\omega) = V_0 \cos \omega t \tag{1}$$

And to measure the current response, which is expressed as:

$$I(\omega) = I_0 \cos(\omega t + \varphi) \tag{2}$$

The impedance Z is a complex number that is defined as the opposition offered by a conductor to a current generated by applying an alternating voltage, and is represented as ratio between applied potential V(ω) and current obtained I(ω), that is to say:

$$Z(\omega) = \frac{\hat{V}(\omega)}{\hat{I}(\omega)} \tag{3}$$

Remembering that:

$$\cos(\omega t + \varphi) = Re\left\{e^{[i(\omega t+\varphi)]}\right\} \tag{4}$$

Expressions for current and voltage can be rewritten as:

$$V(t) = Re\ (V\ e^{i\omega t}) \tag{5}$$

$$I(t) = Re\ (I\ e^{i\omega t}) \tag{6}$$

Where: $I = I_0\ e^{i\varphi}$ and $V = V_0$.

If we consider relationships between voltage and current for a resistor R, an inductor L and a capacitor C (passive elements of a basic circuit):

$$\begin{cases} V(t) = R\,I(t) \rightarrow V_R = R\,I_R \\ V(t) = L\,\dfrac{dI(t)}{dt} \rightarrow V_L = i\omega L\,I_L \\ I(t) = C\,\dfrac{dV(t)}{dt} \rightarrow V_C = \dfrac{1}{i\omega C}\,I_C \end{cases} \tag{7}$$

From Eq. (3) it is possible to find impedance contribution to each passive circuit element:

$$\begin{cases} Z_R = R \\ Z_L = i\omega L \\ Z_C = \dfrac{1}{i\omega C} \end{cases} \tag{8}$$

Since impedance is a complex quantity, it can be expressed as:

$$Z = R + i\,X \tag{9}$$

Where $R = Re(Z)$ is the resistance, and $X = Im(Z)$ is defined as the reactance, from Eq. (8) it can see that there are two reactances: inductive and capacitive reactance.

In this paper, electrical transport properties of perovskite solar cells with planar architecture were evaluated using impedance spectroscopy, especially the active layer thickness effect on solar cell efficiency.

II. Experimental

The analysis was performed by measuring the impedance spectrum of the solar cell followed by a theoretical adjustment of this spectrum, using an equivalent circuit model as shown in Fig. 1, which has been used by other authors to describe processes of electric transport in solar cells with interplanar structure and based on perovskite [6, 7].

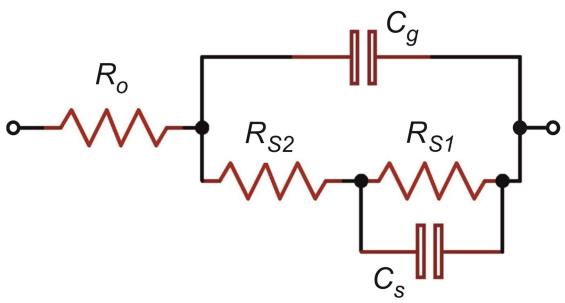

Fig. 1. Circuit used to simulate impedance spectra. R_0 is the series resistance of the device associated with ohmic contribution of wires and contacts, resistors R_{S1} and R_{S2} are related to the current flow of surface recombination, C_g is the capacitance associated with the dielectric response of the device and C_S is the capacitance associated with the accumulation of load at the interfaces.

Equivalent circuit elements represent electrical processes that are carried out mostly in the active layer of the cell and in its different interfaces. R_0 is the series resistance of the device associated with the ohmic contribution of the contacts and cable, the resistors R_{S1} and R_{S2} are resistances associated with the flow of linear recombination current at high and low frequencies respectively.

Capacitive elements each have a different interpretation: C_S is associated with the accumulation of charge at the interfaces, mainly ETL/MAPI interface [6], and responds to the mechanisms that govern the operation of the cell at low frequencies (~ 1 Hz). As perovskite solar cells contain different types of charge carriers (ionic and electronic), the electronic charge is what produces the photocurrent while the ionic charge is not usable and is invested in the degradation of the material, as it migrates (low the effect of the internal electric field) of the methylammonium cation contained in the active layer towards the ETL/MAPI interface, C_S then appears as a consequence of the accumulation of ionic charge at said interface [6, 7].

Finally, C_g is related to the dielectric response of active layer and dominates the capacitive response at high frequencies (> 1 kHz) of the spectrum, the capacitance C_g is given by:

$$C_g = \frac{\varepsilon\,\varepsilon_0}{d} \tag{10}$$

Where ε is the perovskite layer dielectric constant, d the layer thickness and ε_0 is the vacuum permittivity.

The measurements were made in the frequency range from 0.1 to 1×10^7 Hz, using a Potentiostat IVIUM Compacpstat Multiwave 32, capable of generating a sinusoidal signal of electric potential of variable frequency on the material studied, and recording the response in current. And for the simulation, the "EIS Spectrum Analyzer" program was used, which allows the design of equivalent circuits and subsequent adjustment of parameters from experimental curves. At the end of the adjustment, specific values of capacitance, resistance, inductors and constant phase elements are obtained.

For the analysis, perovskite solar cells with regular planar architecture are manufactured: FTO/ZnO/MAPI/P_3HT/Au following the procedure described in the reference [8], maintaining the same synthesis parameters for all layers and varying only the thickness of the active layer between 300 and 600 nm, since this is a parameter that significantly affects the cell efficiency.

III. Results

Figure 2 shows impedance spectra, corresponding to measurements made on solar cells with FTO/ZnO/MAPI/P_3HT /Au architecture, taking into account three different active layer thicknesses: 300, 450 and 600 nm.

Table 1 shows resistance and capacitance values calculated from theoretical simulation of the spectra (see Fig. 2), using mathematical tools that allow an adjustment of the experimental impedance curve with the simulated a from the equivalent circuit of Figure 1 and with help of "EIS Spectrum Analyzer" program.

Results of Table 1 reveal that C_g presents values of the order of nano-farads, on the other hand, C_S is significantly higher reaching values of 1.88 µF, a result that can be interpreted in terms of an increase in the accumulation of carriers majority (holes) in the ETL(ZnO)/perovskite interface.

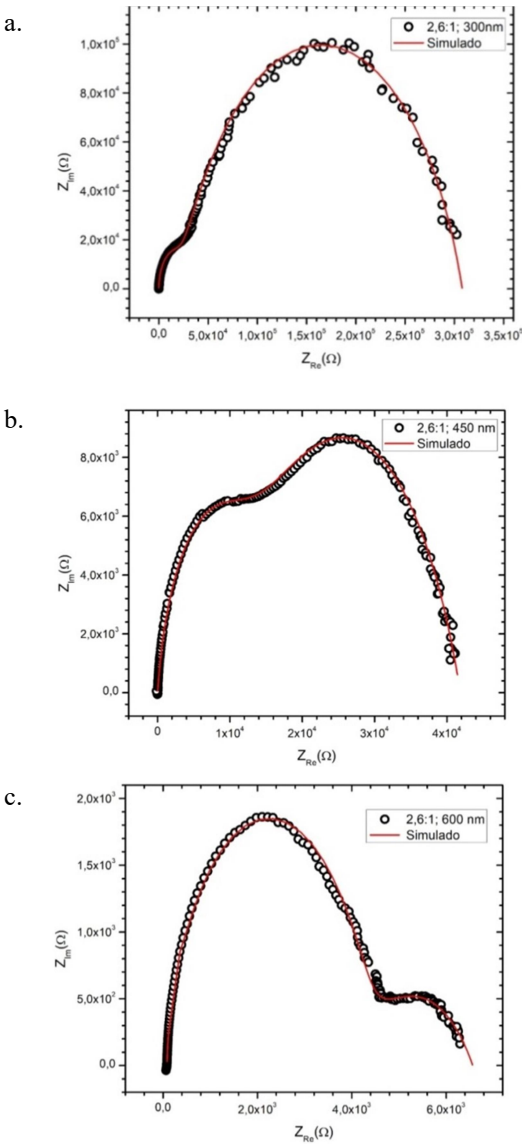

Fig. 2. Experimental and simulated impedance spectrum (red continuous line) of a solar cell manufactured with FTO/ZnO/MAPI/P_3HT/Au architecture, where the active layer is deposited with different thickness, (a) 300 nm, (b) 450 nm and (c) 600 nm.

TABLE 1. Resistance and capacitance values obtained from the adjustment between experimental and simulated impedance curves.

MAPI thickness (nm)	$R_{S1}(\Omega)$	$R_{S2}(\Omega)$	C_g(μF)	C_S(μF)
300	2.98E5	2.75E4	4.03E-3	1.66E-1
450	2.76E4	1.42E4	1.60E-2	9.19E-1
600	2.31E3	4.17E3	3.98E-3	1.88

The energy band diagram shown in Fig. 3, indicates the charge accumulation layer that induces an upward deflection of the energy bands with an extension equal to the Debye length (L_D), which is given by:

$$L_D = \left[\frac{\varepsilon\,\varepsilon_0\,k_B\,T}{q^2\,\rho_0}\right]^{1/2} \quad (11)$$

Where $k_B\,T$ is the thermal energy and ρ_0 the density of major carriers that corresponds to the density of donor impurities that is typically of the order of 10^{17} cm^{-3}; therefore $L_D \sim 10$ nm.

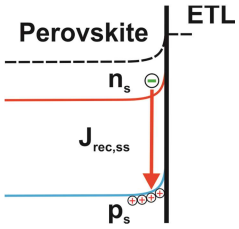

Fig. 3. Energy bands diagram of the zone of charge accumulation in the perovskite, near the contact (ETL/perovskite layer).

IV. CONCLUSIONS

Through simulations of the impedance curves, it was possible to model the electrical behavior of the cells, where simulated circuit elements values were found: R_0, R_{S1}, R_{S2}, C_g and C_S. Both resistive elements appear in some way related to the C_S capacitance by a common mechanism. In general, the resistance at low frequencies R_{S1} has higher values than the component R_{S2} at high frequencies and since these have an inverse relationship with the recombination current $J_{rec,s}$ we can say that photocurrent losses by recombination are greater at high frequencies.

ACKNOWLEDGMENT

This work was supported by Colciencias (Contract #184/2016) and Universidad Nacional de Colombia, Sede Bogotá, Facultad de Ciencias, Departamento de Física, Grupo GMS&ES, K30 #45-03, Bogotá DC, Colombia.

REFERENCES

[1] A. F. Loaiza, Preparación de materiales fotovoltaicos orgánicos y estudio de propiedades de transporte eléctrico usando espectroscopia de impedancia, Bogotá: Universidad Nacional de Colombia, 2014.

[2] I. Mora-Seró, G. Garcia-Belmonte, P. Boix, M. A. Vázquez y J. Bisquert, «Impedance spectroscopy characterisation of highly efficient silicon solar cells under different light illumination intensities,» *Energy Environ. Sci.,* vol. 2, pp. 678-686, 2009.

[3] F. Fabregat-Santiago, G. Garcia-Belmonte, I. Mora-Seró y J. Bisquert, «Characterization of nanostructured hybrid and organic solar cells by impedance spectroscopy,» *Phys. Chem. Chem. Phys.* , nº 13, pp. 9083-9118, 2011.

[4] C. Alexander y M. Sadiku, Fundamentos de circuitos eléctricos, México, D. F.: McGraw-Hill Interamericana, 2006.

[5] J. Bisquert y F. Fabregat-Santiago, «Impedance Spectroscopy: A general introduction and Application to dye-sensitized solar cells,» de *Dye-sensitized solar cells*, Lausanne, EPFL Press, 2010, pp. 457-554.

[6] I. Zarazúa, G. Han, P. P. Boix, S. Mhaisalkar, F. Fabregat-Santiago, I. Mora-Sero, J. Bisquert y G. Garcia-Belmonte, «Surface recombination and collection efficiency in perovskite solar cells from impedance analysis,» *Journal of Physical Chemical Letters,* vol. 11, pp. 1948-1958, 2016.

[7] B. Suarez, V. Gonzalez-Pedro, T. S. Ripolles, R. S. Sanchez, L. Otero y I. Mora-Sero, «Recombination study of combined halides (Cl, Br, I) perovskite solar cells,» *Journal of Physical Chemical Letters,* vol. 5, pp. 1628-1635, 2014.

[8] M. A. Reinoso, C. Otálora y G. Gordillo, «Improvement of the properties of CH3NH3PbI3 thin films prepared by sequential evaporation using an advanced control system,» *Materials,* vol. 12, nº 1394, pp. 1-17, 2019.